



Original Research

# Influence of the incorporation of marine spongin into a Biosilicate®: an *in vitro* study

K. R. Fernandes<sup>1</sup> · J. R. Parisi<sup>1</sup> · A. M. P. Magri<sup>2</sup> · H. W. Kido<sup>2</sup> · P. R. Gabbai-Armelin<sup>2</sup> · C. A. Fortulan<sup>3</sup> · E. D. Zanotto<sup>4</sup> · O. Peitl<sup>4</sup> · R. N. Granito<sup>2</sup> · A. C. M. Renno<sup>2</sup>

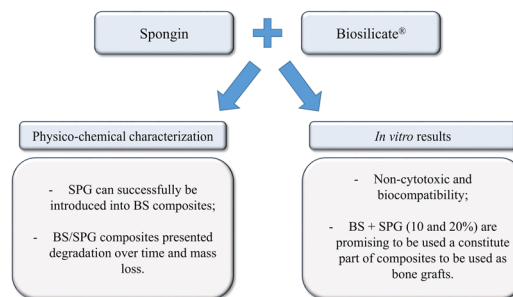
Received: 28 August 2018 / Accepted: 10 May 2019 / Published online: 24 May 2019  
© Springer Science+Business Media, LLC, part of Springer Nature 2019

## Abstract

The combination of different biomaterials can be a promising intervention for the composites manufacture, mainly by adding functional and structural characteristics of each material and guarantee the advantages of the use of these composites. In this context, the aim of this study was to develop and evaluated the influence of the incorporation of marine spongin (SPG) into Biosilicate® (BS) in different proportions be used during bone repair. For this purpose, it was to develop and investigate different BS/SPG formulations for physico-chemical and morphological characteristics by pH, loss mass, Fourier transform infrared spectrometer (FTIR) and scanning electron microscope (SEM) analysis. Additionally, the influence of these composites on cell viability, proliferation, and alkaline phosphatase (ALP) activity were investigated. The results revealed that the pH values of all BS groups (with or without SPG) increased over time. A significant mass loss was observed in all composites, mainly with higher SPG percentages. Additionally, SEM micrographies demonstrated fibers of SPG into BS and material degradation over time. Moreover, FTIR spectral analysis revealed characteristic peaks of PMMA, BS, and SPG in BS/SPG composites. BS/SPG groups demonstrated a positive effect for fibroblast proliferation after 3 and 7 days of culture. Additionally, BS and BS/SPG formulations (at 10% and 20% of SPG) presented similar values of osteoblasts viability and proliferation after 7 days of culture. Furthermore, ALP activity demonstrated no significant difference between BS and BS/SPG scaffolds, at any composition. Based on the present *in vitro* results, it can be concluded that the incorporation of SPG into BS was possible and produced an improvement in the physical-chemical characteristics and in the biological performance of the graft especially the formulation with 80/20 and 90/10. Future research should focus on *in vivo* evaluations of this novel composite.

## Graphical Abstract

Influence of the incorporation of marine spongin into a Biosilicate®: an *in vitro* study



✉ K. R. Fernandes  
kellyrf10@yahoo.com.br

<sup>1</sup> Department of Physiotherapy, Federal University of São Carlos (UFSCar), São Carlos, SP, Brazil

<sup>2</sup> Department of Biosciences, Federal University of São Paulo (UNIFESP), Santos, SP, Brazil

<sup>3</sup> Department of Mechanical Engineering, São Carlos School of Engineering, São Carlos, SP, Brazil

<sup>4</sup> Department of Materials Engineering, Vitreous Materials Laboratory (LaMaV), Federal University of São Carlos (UFSCar), São Carlos, SP, Brazil

## 1 Introduction

Biomaterial based bone grafts represent a very promising therapeutical intervention to be used for dental and orthopedic applications [1]. It is well known that grafts manufactured from autologous bone produces the best clinical outcomes and are considered the gold standard, being able of providing osteogenic progenitor cells and growth factors for bone cell differentiation and lacking immune-related complications [2]. However, their use involve the need of an extra surgical intervention and considerable donor site morbidity associated with the harvest [3, 4]. In this context, synthetic biomaterials have been emerging as an alternative for engineered designed bone grafts, being tailored to present handling properties, good osteogenic performance, stimulating cell proliferation and osteogenesis and appropriate resorption rate [5].

Bioactive glasses and glass-ceramics (including Biosilicate<sup>®</sup>) are one of the most promising biomaterials for bone tissue engineering [6–14]. They are a class of synthetic silica-based bioactive materials with the ability to bond to bone tissue, forming an active apatite layer on their surface, which acts as a template for newly bone formation [6, 15, 16]. Especially, Biosilicate<sup>®</sup> (BS), a particular composition of a group of fully crystallized glass-ceramics of the  $\text{Na}_2\text{O}-\text{CaO}-\text{SiO}_2-\text{P}_2\text{O}_5$  system, has been demonstrating very positive effects on bone metabolism and on the acceleration of fracture healing.

However, in specific critical situations such as bone fractures with poor vascularization or in the presence of diseases such as osteoporosis, the osteoconductive properties of BS may not be sufficient to induce bone ingrowth and fracture consolidation. Consequently, combining two or more biomaterials, with different characteristics has been emerging as a possible alternative to obtain more effective bone grafts [17–19]. Thus, the association of BS (which can represent the bone mineral part) with an organic part (such as collagen), may constitute a graft with improved biological properties, being a more suitable material to be used as bone substitutes.

Additionally, different sources of collagen to be used in the tissue engineering field have been explored by many authors such as collagen from marine sponges or spongin (SPG) [20–22]. It has been demonstrated that SPG shows a similar composition to type XIII vertebrate collagen [23, 24] and it seems to be able of accelerating osteoblast cell proliferation in in vitro studies, showing an osteogenic potential [23–25].

As it is of high demand the development of bone substitutes with a higher osteogenic potential, it was hypothesized that the addition of SPG to BS might offer a very innovative way of improving the biological performance. The introduction of SPG was designed to integrate its high

bioactivity rate to the bioactive material, increasing the osteogenic potential. Thus, the aim of the current study was to investigate different BS/SPG formulations for physico-chemical and morphological characteristics and the influence of these composites on cell viability and proliferation and alkaline phosphatase (ALP) activity in in vitro studies.

## 2 Materials and methods

### 2.1 Materials

BS parent glass used in the present study was a fully crystallized bioactive glass ceramic of the quaternary  $\text{P}_2\text{O}_5-\text{Na}_2\text{O}-\text{CaO}-\text{SiO}_2$  system (patent application WO2004/074199). BS (particle size 250–1000  $\mu\text{m}$ ) was provide by Vitreous Materials Engineering, Federal University of São Carlos, São Carlos, SP, Brazil). Additionally, Poly (methyl methacrylate) (PMMA, particle size: 15  $\mu\text{m}$ ) and methyl methacrylate (MMA, purity: 99.09%) were provided by VIPI Produtos Odontológicos (Pirassununga, São Paulo, Brazil). Both polymer and monomer were utilized exclusively to aggregate the BS and SPG. Carboxymethyl cellulose (CMC), density 1.59  $\text{g}/\text{cm}^3$ , was provided by Sigma Aldrich (Missouri, USA) and distilled water to provide crosslinked and interconnected porosity.

### 2.2 SPG

*Aplysina fulva* marine sponge was used for the SPG extraction. Samples were collected from high hydrodynamism coasts, in the intertidal zone, in Praia Grande (23o49'23.76 "S, 45o25'01.79" W, São Sebastião, Brazil) and in Araçá Bay area (23o81'73.78 "S, 45o40'66.39 "W, São Sebastião, Brazil). SPG was isolated by a previously described method with some modifications [26]. Briefly, the collection was performed using a scalpel blade. The samples were immediately washed with sea water, placed in containers containing sea water, and transported to the laboratory in thermal boxes. Three washing steps were performed in Milli-Q water to remove cell debris and immediately after the samples were stored in a freezer at  $-20\text{ }^\circ\text{C}$ . For the extraction of SPG, species of marine sponges were cut into small pieces and placed separately in Tris-HCl buffer (100 mM, pH 9.5, 10 mM EDTA, 8 M urea, 100 mM 2-mercaptoethanol). After, the pH was adjusted to 9 with the use of the NaOH solution. Then, this solution was transferred into a stirred beaker during 24 h. After, the solution was centrifuged (5000 g; 5 min and  $2\text{ }^\circ\text{C}$ ). The pellet was discarded, and the supernatant was removed for analysis. The pH was adjusted again to 4 with the use of acetic acid solution. In this stage, it was possible to observe the formation of the precipitate. This precipitate was

**Table 1** Experimental formulations of composites expressed in grams (g)

Groups	PMMA (g)	MMA (g)	BS (g)	SPG (g)	CMC (g)	Water (g)
PMMA	0.472	0.944	0	0	0.043	0.565
BS	0.236	0.472	0.560	0	0.043	0.565
SPG	0.236	0.472	0	0.268	0.043	0.565
BS/SPG 90/10	0.236	0.472	0.295	0.127	0.043	0.565
BS/SPG 80/20	0.236	0.472	0.368	0.092	0.043	0.565
BS/SPG 70/30	0.236	0.472	0.455	0.051	0.043	0.565

resuspended in Milli-Q water, and after it was centrifuged again. The solution was lyophilized for preservation of the SPG [26].

### 2.3 Preparation of scaffolds

For this study, 5 different scaffolds were used manufactured with different materials and formulations: PMMA; BS; BS/SPG 90/10; BS/SPG 80/20 and BS/SPG 70/30. The lowest amount of PMMA sufficient to aggregate the different materials was used. In addition, CMC was used as a porogenic material and the quantity utilized for this component in each composite is toward inducing porosity of 60% [27–29]. All materials (i.e., PMMA, BS, SPG, and CMC) in powder, and distilled H<sub>2</sub>O were weighed and mixed in a silicone container using a spatula, at the different proportions corresponding to each group (Table 1). After that, distilled water was added, the combination was mixed, followed by the addition of MMA monomer (to produce the crosslink). Then, the mixture was rapidly transferred to a silicon mold of 6 mm diameter × 2 mm height. Subsequently, the molds were sealed and submitted to a pressure air chamber at 0.6 MPa for 30 min. Afterwards, the molds were vacuum dried (10<sup>-3</sup> Torr) for 15 min and the composites were removed from the silicon molds, packaged, and sterilized by ethylene oxide (Acecil, Campinas, SP, Brazil).

### 2.4 Physicochemical tests

#### 2.4.1 In vitro degradation

Degradation of the scaffolds was studied by evaluating pH and mass loss after 0, 3, 7, 14, and 21 days of immersion in phosphate buffered saline (PBS). Composite formulations were prepared and individually weighted. Samples ( $n = 3$ ) were immersed in 3 mL of PBS (10 mM and pH = 7.4) and incubated at 37 °C in a water bath on a shaker table. For each experimental period, samples were removed from the solution and the pH was measured ( $n = 3$ ) using a pH electrode (Orion Star A211, Thermo Scientific, Massachusetts, USA). Moreover, the scaffolds were vacuum dried overnight before measuring the mass. Mass loss was evaluated comparing the initial and final mass for each individual sample.

#### 2.4.2 FTIR

Infrared spectra of the PMMA; BS; BS/SPG 90/10; BS/SPG 80/20 and BS/SPG 70/30 were obtained by a reflection of FTIR (Bomem Michelson Series at 400 a 4000 cm<sup>-1</sup> interval with 4 cm<sup>-1</sup> resolution).

#### 2.4.3 SEM

The morphology of the preset scaffolds were evaluated by SEM (Le0 440, Carl Zeiss, Jena, Germany) operating with a 10 keV electron beam. The surface morphology and degradation behavior were analyzed before incubation and after 7 and 21 days of incubation in PBS. To obtain SEM images, samples were mounted on aluminum stubs using carbon tape and sputter-coated with gold prior to examination.

### 2.5 In vitro study

#### 2.5.1 Cell culture

In this study two cell lines were used, mouse calvaria-derived MC3T3-E1 subclone 14 preosteoblastic cells (Bank of Cells of Rio de Janeiro, Rio de Janeiro, RJ, Brazil) and murine fibroblasts cells (L929) (ATCC CCL-1, passage 5) (Bank of Cells of Rio de Janeiro, Rio de Janeiro, RJ, Brazil). Cells were cultured in Dulbecco's Modified Eagle Medium (DMEM, Vitrocell, Campinas, SP, Brazil) for L929 and alpha Minimal Essential Medium ( $\alpha$ -MEM; Vitrocell, Campinas, Brazil) for MC3T3. Both medias were supplemented with 10% fetal bovine serum (Vitrocell, Campinas, SP, Brazil) and 1% antibiotic–antimycotic solution (Vitrocell, Campinas, SP, Brazil) and the cells were maintained at 37 °C in a humidified atmosphere of 5% CO<sub>2</sub>. For cell viability and cell proliferation: cells were seeded at 1 × 10<sup>4</sup> cells/cm<sup>2</sup> in 48-well plate (Kasvi, Curitiba, PR, Brazil) with extract of PMMA, BS, BS/SPG 90/10, BS/SPG 80/20, and BS/SPG 70/30 containing 500  $\mu$ l of composites extracts for 1, 3, and 7 days. For osteogenic differentiation by ALP activity: cells were seeded at 1 × 10<sup>4</sup> cells/cm<sup>2</sup> in 24-well plate (Kasvi, Curitiba, PR, Brazil) with extract of PMMA, BS, BS/SPG 90/10, BS/SPG 80/20, and BS/SPG

70/30 containing 1 ml of composites extracts for 14 and 21 days. The medium was refreshed every 2–3 days. In vitro biological response analyzes were performed in triplicate ( $n=4$ ). To obtain the extracts, samples were immersed and incubated in their respective media (50 mL/g) at 37 °C in a humidified atmosphere of 5% CO<sub>2</sub> for 7 days. Then, the medium was filtered (0.22 μm, Kasvi) and used for the in vitro experiments. For the control groups, only each medium without extract was used.

### 2.5.2 Cell viability

The cell viability was evaluated by alamarBlue® assay (Bio-Rad AbD Serotec GmbH, Puchheim, Germany). Additionally, cell proliferation was quantified using a QuantiFlour® dsDNA System Kit (Promega, Madison, WI, USA) [30]. Therefore, the cell lineages were cultivated into extracts of the materials. MC3T3 and L929 cells were cultivated at a density of  $1 \times 10^4$  cells per cm<sup>2</sup> in 48-well plates containing 500 μl of composites extracts, that was previously collected, and the cells were cultivated for 1, 3, and 7 days. For cell viability, 50 μl of alamarBlue® solution was added to each well, and the plate was stored in the dark at 37 °C during 4 h in a cell culture incubator. After this period, 200 μl of the samples were transferred to a 96-well plate and measurements were performed using a microplate reader (Bio-Tek Instruments, Inc.) at 570 nm.

### 2.5.3 Cell proliferation

Subsequently, the alamarBlue® solution in contact with cells was washed away twice using PBS and the same well-plate, at each experimental period. After, 500 μl of Milli-Q water was added in each well and was stored in the freezer until the analysis of DNA quantification by PicoGreen assay (QuantiFluor® dsDNA quantification kit; Promega, Leiden, The Netherlands). After 2 freeze-thaw cycles (−80 °C and 25 °C), 100 μl of freshly made working solution was added into each well which contained 100 μl of sample or DNA standard, and the plate was stored in the dark for 5 min. Finally, the fluorescent signal (485/20 excitation and 530/25 emission) was read using a microplate reader (SpectraMax® M5, Molecular Devices, California, USA).

### 2.5.4 ALP activity

ALP activity was performed a colorimetric assay using a 5 nM p-nitrophenyl phosphate (4-NP) (Sigma-Aldrich, St. Louis, MO, USA). First, 80 μl sample or standard (serial dilutions of 4-nitrophenol at the concentrations of 0–25 nM) plus 20 μl buffer solution (0.5 M 2-amino-2-methyl-1-propanol) were added into 96 well-plate. Then, 100 μl substrate solution (p-nitrophenyl phosphate) was added to all the

wells and incubated at 37 °C for 1 h. To stop the reaction was deposited 100 μl of 0.3 M NaOH and the ALP activity was measure in a spectrophotometer (Bio-Tek Instruments) at 405 nm.

## 2.6 Statistical analysis

Data were expressed as mean ± standard deviation. The normality of all variable's distribution was verified using the Shapiro–Wilk *W* test. For the variable that exhibited normal distribution, comparisons among the groups were made using one-way analysis of variance (ANOVA) with post hoc Tukey Multiple Comparisons test. For the variable that exhibited non-normal distribution, Kruskal Wallis tests were used. GraphPad Prism version 6.01 was used to carry out the statistics analysis. Values of  $p < 0.05$  were considered statistically significant.

## 3 Results

### 3.1 In vitro degradation

Figure 1 shows the results of the pH measurement during degradation in PBS. pH of PMMA group showed constant values over time (7.34–7.30). Furthermore, an increase in pH was observed after 3 days of incubation for BS, BS/SPG 90/10, BS/SPG 80/20, and BS/SPG 70/30 (pH values between 10.05 and 10.32). The increase in pH value continuous increasing for all BS groups until the last experimental period (for BS on days 7, 14, and 21 pH values were 10.64; 11.01 and 11.36, respectively), (for BS/SPG 90/10 on days 7, 14, and 21 pH values were 10.55; 10.52 and 10.7, respectively), (for BS/SPG 80/20 on days 7, 14, and 21 pH values were 10.57; 10.8 and 11.18, respectively) and (for BS/SPG 70/30 on days 7, 14, and 21 pH values were 10.51; 10.38 and 11.41, respectively). Furthermore, pH values of PMMA groups for all experimental periods were

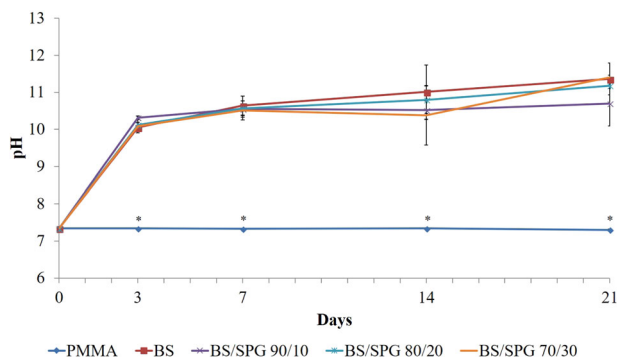


**Fig. 1** pH change after incubation in PBS for PMMA; BS; SPG; BS/SPG 90/10; BS/SPG 80/20 and BS/SPG 70/30 after 3, 7, 14, and 21 days. Values represent the mean of three samples. \* $p < 0.05$

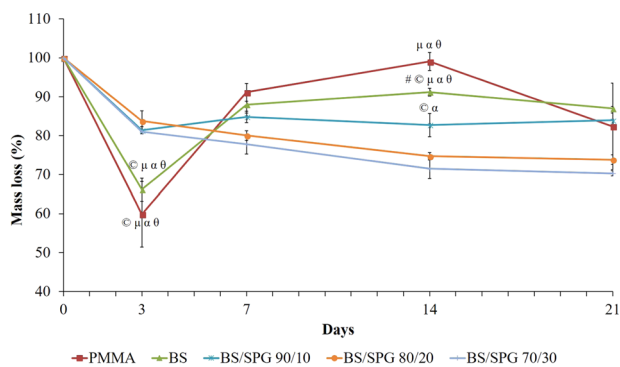


**Fig. 2** Mass loss (%) measurements for PMMA; BS; BS/SPG 90/10; BS/SPG 80/20 and BS/SPG 70/30. Values represent the mean of three samples. **Day 3:**  $\mu$  BS/SPG 90/10 versus PMMA and BS;  $\alpha$  BS/SPG 80/20 versus PMMA and BS;  $\theta$  BS/SPG 70/30 versus PMMA and BS. **Day 7:**  $\mu$  BS/SPG 90/10 versus PMMA and BS/SPG 70/30;  $\alpha$  BS/SPG 80/20 versus PMMA and BS;  $\theta$  BS/SPG 70/30 versus PMMA and BS. **Day 14:**  $\mu$  BS/SPG 90/10 versus PMMA and BS;  $\alpha$  BS/SPG 80/20 versus PMMA and BS;  $\theta$  BS/SPG 70/30 versus PMMA, BS and BS/SPG 90/10. **Day 21:** # BS versus BS/SPG 70/30

lower compared to the other groups ( $p < 0.0001$ ). No other significant difference was observed.

### 3.2 Mass loss

Mass loss (%) measurements upon soaking in PBS are presented in the Fig. 2. In the first period analyzed, all composites analyzed demonstrated mass loss, mainly in the PMMA and BS, which reached values of 59.8% and 66.1%, respectively. Statistical differences were observed after 3 days of immersion, when a higher mass loss was observed in PMMA compared to BS/SPG 90/10 ( $p = 0.0006$ ), BS/SPG 80/20 ( $p = 0.0003$ ), and BS/SPG 70/30 ( $p = 0.0007$ ). Additionally, BS showed a higher mass loss compared to BS/SPG 90/10 ( $p = 0.0082$ ), BS/SPG 80/20 ( $p = 0.003$ ), and BS/SPG 70/30 ( $p = 0.0097$ ).

After 7 days of incubation, PMMA showed a lower mass loss compared to BS/SPG 90/10 ( $p = 0.0214$ ), BS/SPG 80/20 ( $p = 0.0004$ ), and BS/SPG 70/30 ( $p < 0.0001$ ). Similar behavior was also observed for BS compared to BS/SPG 80/20 ( $p = 0.0048$ ) and BS/SPG 70/30 ( $p = 0.0008$ ). In this same period, it was observed a higher mass loss in BS/SPG 90/10 compared to BS/SPG 70/30 ( $p = 0.00110$ ). After 14 days of incubation, PMMA showed a higher mass loss compared to BS ( $p = 0.0078$ ), BS/SPG 90/10 ( $p < 0.0001$ ), BS/SPG 80/20 ( $p < 0.0001$ ), and BS/SPG 70/30 ( $p < 0.0001$ ). Additionally, in the same period, BS showed similar results compared to BS/SPG 90/10 ( $p = 0.0045$ ), BS/SPG 80/20 ( $p < 0.0001$ ) and BS/SPG 70/30 ( $p < 0.0001$ ). The BS/SPG 90/10 demonstrated a lower mass loss compared to BS/SPG 80/20 ( $p = 0.0066$ ) and BS/SPG 70/30 ( $p = 0.0005$ ). In the last experimental period (21 days), a higher mass loss was observed for BS/SPG 70/30 compared to BS ( $p = 0.0165$ ).

### 3.3 SEM

Figure 3 shows the SEM images of composites with and without immersion. For PMMA samples, microspheres were observed in all photomicrographs, becoming more evident after immersion, with similar aspects for both 7 and 21 days. Furthermore, it was possible to observe the glass-ceramic structure in the SEM images of BS scaffolds (without immersion), with some particles of PMMA. After 7 and 21 days of immersion, it was still possible to identify BS particles and PMMA microspheres, but with a less homogeneous appearance however, evidences of material degradation over time can be noticed. For all BS/SPG composites, fibers of SPG can be observed, forming a net around the BS, and the PMMA microspheres. After immersion, signs of degradation of BS/SPG composites were observed, with the formation of pores.

### 3.4 FTIR

Chemical compositions of the composites can be observed in the FTIR spectra in Fig. 4. PMMA spectra reflect the presence of the C–O bonds within the polymer; can be observed bands can be observed in the following regions: 3050–2999  $\text{cm}^{-1}$  (CH stretching vibration); 1730  $\text{cm}^{-1}$  (CO double bond stretching vibration); 1260–1040  $\text{cm}^{-1}$  (COC single bond stretching vibration) and 808–960  $\text{cm}^{-1}$  (COC single bond deformation vibration). BS spectrum showed a band in 1100–900  $\text{cm}^{-1}$  ( $\text{SiO}_2$  and  $\text{PO}_4^{-3}$ ) and 500–610  $\text{cm}^{-1}$  (P–O and Si–O–Si). SPG spectrum demonstrated bands in the following regions: 3500  $\text{cm}^{-1}$  (O–H stretch); 3200  $\text{cm}^{-1}$  (asymmetric and symmetric axial deformations of NH); 1700–1600  $\text{cm}^{-1}$  (C=O axial deformation); 1400  $\text{cm}^{-1}$  (interaction between the angular deformation of N–H and the axial deformation of C–N). BS/SPG 90/10; BS/SPG 80/20 and BS/SPG 70/30 spectra can verify the characteristic bands of PMMA, BS, and SPG in different proportions.

### 3.5 Cell viability

For L929 cell viability, no statistical difference was observed among the groups after 1 and 3 days of culture (Fig. 5). On day 7, statistically higher values of L929 viability were observed for Control, PMMA, BS/SPG 90/10; BS/SPG 80/20; BS/SPG 70/30 compared to BS ( $p = 0.0003$ ;  $p = 0.0025$ ;  $p = 0.0108$ ;  $p = 0.0316$ ;  $p = 0.0403$ , respectively). No other difference was observed.

### 3.6 MC3T3

The AlamarBlue® assay of MC3T3 revealed that, 1 day after seeding, Control and PMMA group showed higher cell



**Fig. 3** SEM representative micrographs of cross-sections of PMMA; BS; BS/SPG 90/10; BS/SPG 80/20; BS/SPG 70/30 scaffolds of day 0 (before incubation) and after 7 and 21 days of PBS incubation. Pores (yellow arrows); PMMA (yellow arrows head); Biosilicate (#) and SPG (\*) are indicated in the SEM micrographs. Bar represents 200  $\mu\text{m}$

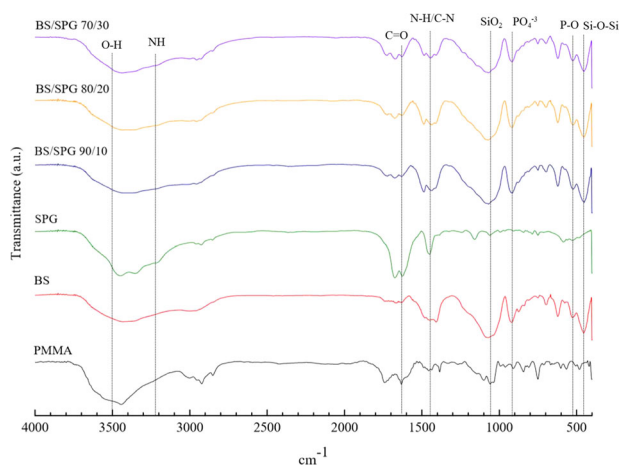
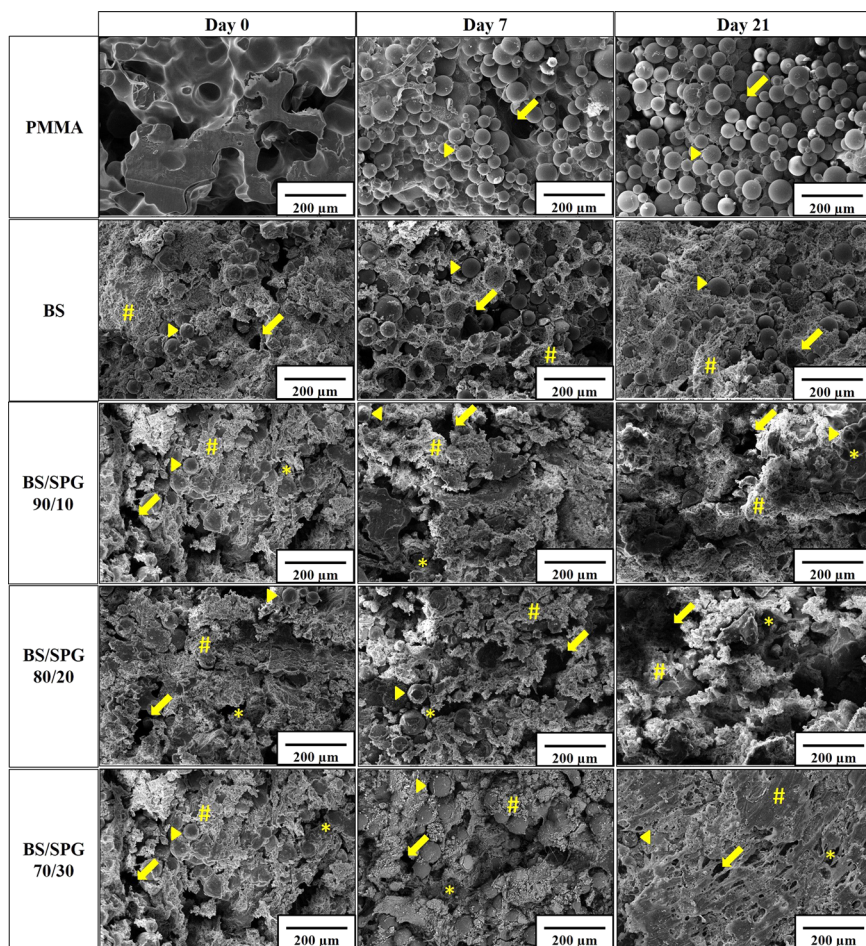


**Fig. 4** FTIR spectra of PMMA, BS, SPG, BS/SPG 90/10, BS/SPG 80/20, and BS/SPG 70/30

viability compared to BS and all the BS/SPG formulations ( $p < 0.0001$ ) (Fig. 6).

After 3 days, Control and PMMA showed a higher percentage of MC3T3 viability when compared to BS and BS/SPG formulations ( $p < 0.0001$ ) (Fig. 6). Furthermore, BS/SPG 90/10 showed a higher cell viability compared to

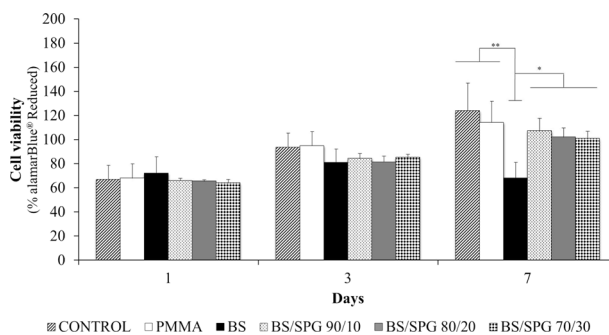


**Fig. 5** Cell viability of L929 by alamarBlue® in solution containing extract of PMMA; BS; BS/SPG 90/10; BS/SPG 80/20; BS/SPG 70/30 after different experimental periods (1, 3, and 7 days) of L929 culture. \* $p < 0.05$ ; \*\* $p < 0.01$  and \*\*\* $p < 0.0001$

BS ( $p = 0.0018$ ) and BS/SPG 70/30 ( $p < 0.0001$ ). Additionally, BS/SPG 80/20 showed a higher value of viability compared to BS/SPG 70/30 ( $p = 0.0042$ ). On day 7, Control and PMMA groups showed higher cell viability compared to BS ( $p = 0.0087$  and  $p = 0.0107$ ); BS/SPG 90/10 ( $p = 0.0028$  and  $p = 0.0035$ ); BS/SPG 80/20 ( $p = 0.0023$  and  $p = 0.0029$ ) and BS/SPG 70/30 ( $p < 0.0001$ , for both). Additionally, BS/SPG 70/30

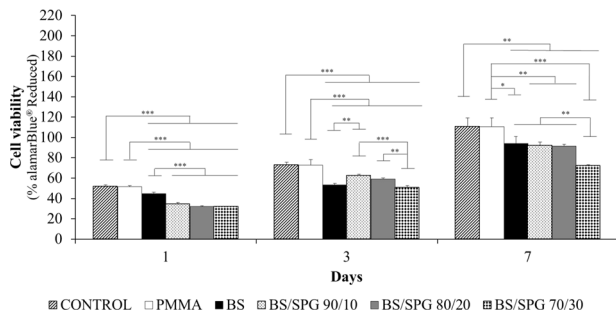


**Fig. 6** Cell viability of MC3T3 by alamarBlue® in solution containing extract of PMMA; BS; BS/SPG 90/10; BS/SPG 80/20; BS/SPG 70/30 after different experimental periods (1, 3, and 7 days) of MC3T3 culture \* $p < 0.05$ ; \*\* $p < 0.01$  and \*\*\* $p < 0.0001$

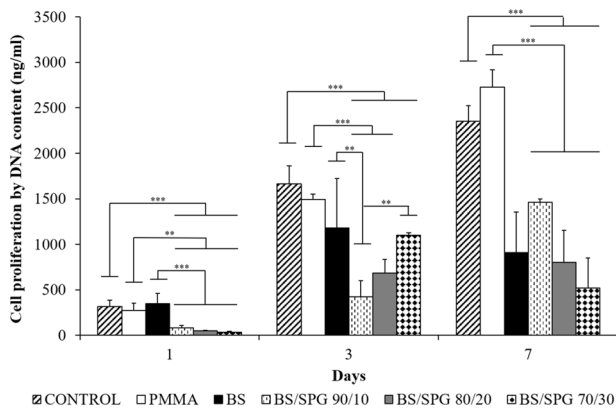


**Fig. 7** Cell proliferation of L929 by DNA content using Control and extract of PMMA; BS; BS/SPG 90/10; BS/SPG 80/20; BS/SPG 70/30 after different experimental periods (1, 3, and 7 days) of culture \* $p < 0.05$ ; \*\* $p < 0.01$  and \*\*\* $p < 0.0001$

demonstrated statistically lower values of MC3T3 viability compared to BS ( $p = 0.0008$ ); BS/SPG 90/10 ( $p = 0.0024$ ) and BS/SPG 70/30 ( $p = 0.0029$ ).

### 3.7 Cell proliferation

Figure 7 demonstrates the values of the DNA content of L929 on days 1, 3, and 7 of cell culture. It was possible to observe that on day 1, Control, PMMA and BS showed a higher cell proliferation compared to BS/PLGA 90/10 ( $p = 0.0008$ ,  $p = 0.0065$ , and  $p = 0.0002$ ); BS/PLGA 80/20 ( $p = 0.0002$ ,  $p = 0.0016$ , and  $p < 0.0001$ ) and BS/PLGA 70/30 ( $p < 0.0001$ ,  $p = 0.0010$ , and  $p < 0.0001$ ).

On day 3, Control showed an increased cell proliferation compared to BS/PLGA 90/10 ( $p < 0.0001$ ); BS/PLGA 80/20 ( $p = 0.0009$ ) and BS/PLGA 70/30 ( $p = 0.0010$ ). Additionally, PMMA demonstrated an increased cell proliferation compared to BS/PLGA 90/10 ( $p < 0.0001$ ); BS/PLGA 80/20 ( $p = 0.0007$ ). Furthermore, BS/PLGA 90/10 reveal a lowest cell proliferation compared to BS ( $p = 0.0006$ ) and BS/PLGA 70/30 ( $p = 0.0012$ ). In the last period analyzed,

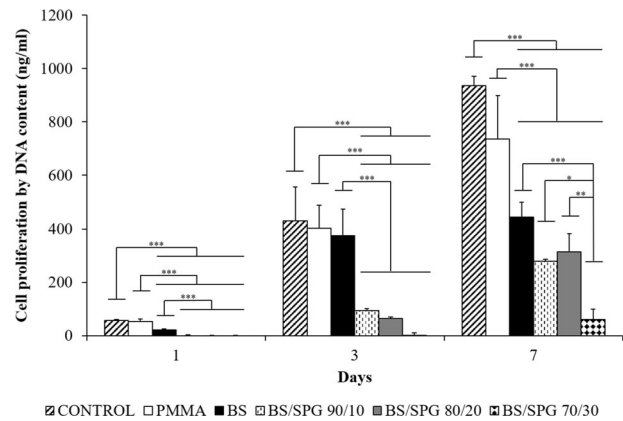


**Fig. 8** Cell proliferation of MC3T3 by DNA content using Control and extract of PMMA; BS; BS/SPG 90/10; BS/SPG 80/20; BS/SPG 70/30 after different experimental periods (1, 3, and 7 days) of culture. \* $p < 0.05$ ; \*\* $p < 0.01$  and \*\*\* $p < 0.0001$

Control and PMMA showed a higher L929 proliferation compared to BS/PLGA 90/10; BS/PLGA 80/20 and BS/PLGA 70/30 ( $p < 0.0001$ ) (Fig. 7).

Figure 8 shows the results of MC3T3 proliferation evaluated by DNA content. On day 1, Control and PMMA showed a higher MC3T3 proliferation compared to other groups ( $p < 0.0001$ ). In addition, BS demonstrated an increase in cell proliferation compared to BS/SPG 90/10; BS/SPG 80/20 and BS/SPG 70/30 ( $p < 0.0001$ ). After 3 days of seeding, it is evident that Control, PMMA, and BS presented a higher cell proliferation compared to BS/SPG 90/10; BS/SPG 80/20 and BS/SPG 70/30 ( $p < 0.0001$ ). After 7 days of culture, Control showed a higher cell proliferation compared to all groups ( $p < 0.0001$ ). Additionally, PMMA demonstrated an increase in MC3T3 proliferation compared to BS ( $p = 0.0006$ ) and BS/SPG 90/10; BS/SPG 80/20 and BS/SPG 70/30 ( $p < 0.0001$ ). Furthermore, BS/SPG 70/30 demonstrated a lower cell proliferation compared to BS ( $p < 0.0001$ ); BS/SPG 90/10 ( $p = 0.0101$ ) and BS/SPG 80/20 ( $p = 0.0025$ ) (Fig. 8).

### 3.8 ALP activity

Figure 9 demonstrates the results for ALP activity evaluation. After 14 days of cell culture, Control showed a higher ALP activity compared to BS ( $p = 0.0003$ ); BS/SPG 90/10 ( $p = 0.0095$ ); BS/SPG 80/20 ( $p = 0.0005$ ) and BS/SPG 70/30 ( $p = 0.0153$ ). Additionally, PMMA demonstrated a higher ALP activity compared to BS ( $p < 0.0001$ ); BS/SPG 90/10 ( $p = 0.0007$ ); BS/SPG 80/20 ( $p = 0.0002$ ) and BS/SPG 70/30 ( $p = 0.0009$ ). As observed in the first period, after 21 days Control and PMMA showed a significant increase in ALP activity compared to BS; BS/SPG 90/10; BS/SPG 80/20 and BS/SPG 70/30 ( $p < 0.0001$ ) (Fig. 9). No other difference was observed.

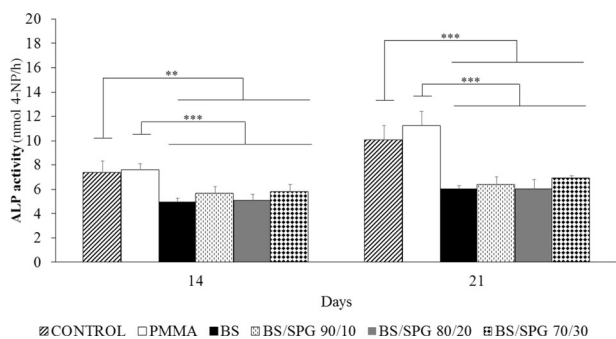


**Fig. 9** ALP activity of MC3T3-E1 in solution containing extract of PMMA; BS; BS/SPG 90/10; BS/SPG 80/20; BS/SPG 70/30 composites after 14 and 21 days of cell culture. \* $p < 0.05$ ; \*\* $p < 0.01$  and \*\*\* $p < 0.0001$

## 4 Discussion

The present work studied the incorporation of marine SPG into BS via evaluation of degradation behavior, morphology of the composites, physico-chemical properties, and in vitro studies. SPG, at different percentages, could be successfully introduced into BS scaffolds, which were easy to handle and presented cohesion in different periods of incubation. pH values of all BS groups (with or without SPG) increased over time, reaching values between 10 and 11. Also, a significant mass loss was observed in the composites, mainly the ones with higher SPG percentages. Additionally, SEM micrographies demonstrated fibers of SPG into BS and material degradation over time. Moreover, FTIR spectral analysis revealed characteristic peaks of PMMA, BS, and SPG in BS/SPG composites. The in vitro studies demonstrated that, for L929 cell lineage, it was observed positive results of BS in cell proliferation on 1 day and similar effects compared to the BS/SPG composites, 3 and 7 days of culture. For osteoblast cell lineage, in vitro studies demonstrated that for BS and BS/SPG formulations (at 10% and 20% of SPG) similar values of cell viability and proliferation were found after 7 days of culture. Furthermore, ALP activity demonstrated no significant difference between BS and BS/SPG scaffolds, at any composition.

pH measurements demonstrated that BS samples produced an alkalization of the immersion medium, with no influence of SPG addition, at any percentage. It is well known that an immediate ion (Si, Na, Ca, and P) release from BS happens when in contact with fluids, resulting in an increased pH [14–16]. Moreover, the lack of influence of SPG in pH corroborates the findings of a previous study of our research group who showed that the incorporation of SPG into Hydroxyapatite materials had no effect in the pH measurements [31].

Mass loss evaluation showed a significant decrease for all the BS/SPG groups compared to BS scaffolds, indicating that the introduction of the organic part accelerates sample

degradation. It is known that an alkalization of the medium is observed after BS immersion mainly due to ions release, which may stimulate the degradation of the BS material [32, 33]. An adequate rate of material dissolution is important for bone healing once is mandatory the liberation of space into the defect to allow tissue ingrowth [34, 35]. These findings corroborate those observed in the SEM analysis, which demonstrated that samples with SPG fibers produced accelerated sample degradation after 7 days of immersion, which progressed until 21 days. Then, it seems that the introduction of SPG into BS constitutes an appropriated strategy for bone tissue engineering purposes, allowing the acceleration of the BS material degradation (demonstrated by the higher mass loss), which consequently, could stimulate the substitution of the material for newly formed bone.

FTIR analysis demonstrated well known representative peaks for PMMA and BS [14, 36]. In addition, BS/SPG groups showed peaks for NH, CH, and OH which characterized the SPG [37].

BS/SPG composites positively influenced fibroblast cell viability after 7 days. This phenomenon may be related to the ion dissolution from the glass ceramic material, which may constitute a stimulus to increase cell metabolism. Moreover, it worth to highlight the BS/SPG (at any formulation) noncytotoxicity once the values found for the fibroblast cells cultivated in the presence of the composites were very close to BS (in the last periods analyzed). All these facts indicate that the samples were biocompatible and created a microenvironment suitable for cell growing. However, SPG did not promote any optimized effects on the biological properties of BS.

For osteoblast cells, it was demonstrated that BS and BS/SPG, at the formulation of 90/10 and 80/20 produced an increase in cell viability and proliferation. Kido et al. [11] and Moura et al. [6] also demonstrated that an increased osteoblast cell proliferation exposed to BS was observed. Moreover, additionally previous studies already established that Bioglass and Col, from different sources, did not present beneficial effects for osteoblastic cell growing and in vivo bone formation [38–41]. Interestingly, the bioinspired scaffold, supposed to mimic natural bone composition (70% of mineral part and 30% of organic part) presented lower values of viability and proliferation compared to the other groups, 7 days of culture. One possible explanation for this behavior may be related to the accelerated material degradation in the samples with the higher percentage of SPG, which could have influenced ion release from BS, constituting an overstimulation for the osteoblast cells. In the current study, contrary results were found with a greater amount of SPG had a negative influence on cell viability and proliferation. These divergent results may be explained by the higher bioactivity of BS compared to hydroxyapatite and



added to the effect of SPG may have been an excessive stimulus to positively stimulate cellular behavior.

Furthermore, ALP is a marker of osteoblast differentiation and activity, consequently in the mineralization of the neoformed tissue [42]. The results of the ALP activity demonstrated no significant difference between BS and BS/SPG groups (at any formulation), showing that the introduction of SPG may not have stimulated early osteoblast maturation.

Our results demonstrated that the incorporation of SPG into BS was possible and produced an improvement in the physical-chemical characteristics, especially regarding to the degradation rate, which may constitute a biological advantage for the material. Moreover, BS/SPG composites, at formulation of 80/20 and 90/10 are noncytotoxic, with similar biological properties compared to BS only (but with no optimized effect over the glass-ceramic). These results encourage us to progress the studies to better understand the interaction of marine collagen associated to bioglasses for bone tissue engineering proposals, mainly in *in vivo* investigations.

## 5 Conclusion

Based on the current study, it can be concluded that SPG can successfully be introduced into BS composites. Additionally, BS/SPG composites presented degradation over time and consequently mass loss. Preliminary cell culture investigations showed that BS/SPG groups demonstrated a positive effect for fibroblast proliferation after 3 and 7 days of culture. Additionally, BS and BS/SPG formulations (at 10% and 20% of SPG) presented similar values of osteoblasts viability and proliferation (after 7 days), showing noncytotoxic and biocompatibility. Summarizing, it can be concluded that these two percentages of SPG (10% and 20%), associated to BS are promising to be used as a constituent part of composites to be used as bone grafts. Further studies should be performed to investigate the effect of SPG into BS samples in *in vivo* models.

**Acknowledgements** The authors would like to acknowledge São Paulo Research Foundation (FAPESP) and Prof. Dr. Márcio Reis Custódio from Department of General Physiology of the Institute of Biosciences (IB-USP) for the assistance with this experiment.

## Compliance with ethical standards

**Conflict of interest** The authors declare that they have no conflict of interest.

**Publisher's note:** Springer Nature remains neutral with regard to jurisdictional claims in published maps and institutional affiliations.

## References

- Amini AR, Laurencin CT, Nukavarapu SP. Bone tissue engineering: recent advances and challenges. *Crit Rev Biomed Eng.* 2012;40:363–408.
- Bhatt RA, Rozental TD. Bone graft substitutes. *Hand Clin.* 2012;28:457–68. <https://doi.org/10.1016/j.hcl.2012.08.001>.
- Dimitriou R, Mataliotakis GI, Angoules AG, Kanakaris NK, Giannoudis PV. Complications following autologous bone graft harvesting from the iliac crest and using the RIA: a systematic review. *Injury.* 2011;42:S3–15. <https://doi.org/10.1016/j.injury.2011.06.015>.
- Verboket R, Leiblein M, Seebach C, Nau C, Janko M, Bellen M, et al. Autologous cell-based therapy for treatment of large bone defects: from bench to bedside. *Eur J Trauma Emerg Surg.* 2018; 44(5):649–65. <https://doi.org/10.1007/s00068-018-0906-y>.
- Bose S, Roy M, Bandyopadhyay A. Recent advances in bone tissue engineering scaffolds. *Trends Biotechnol.* 2012;30:546–54. <https://doi.org/10.1016/j.tibtech.2012.07.005>.
- Moura J, Teixeira LN, Ravagnani C, Peitl O, Zanotto ED, Belotti MM, et al. *In vitro* osteogenesis on a highly bioactive glass-ceramic (Biosilicate). *J Biomed Mater Res Part A.* 2007;82:545–57. <https://doi.org/10.1002/jbm.a.31165>.
- Granito RN, Ribeiro DA, Renno AC, Ravagnani C, Bossini PS, Peitl-Filho O, et al. Effects of biosilicate and bioglass 45S5 on tibial bone consolidation on rats: a biomechanical and a histological study. *J Mater Sci Mater Med.* 2009;20:2521–6. <https://doi.org/10.1007/s10856-009-3824-z>.
- Oliveira FS, Pinfildi CE, Parizoto NA, Liebano RE, Bossini PS, Garcia EB, et al. Effect of low level laser therapy (830 nm) with different therapy regimes on the process of tissue repair in partial lesion calcaneus tendon. *Lasers Surg Med.* 2009;41:271–6. <https://doi.org/10.1002/lsm.20760>.
- Bossini PS, Renno AC, Ribeiro DA, Fangel R, Peitl O, Zanotto ED, et al. Biosilicate(R) and low-level laser therapy improve bone repair in osteoporotic rats. *J Tissue Eng Regen Med.* 2011;5:229–37. <https://doi.org/10.1002/term.309>.
- Matsumoto MA, Caviquioli G, Bigueti CC, Holgado Lde A, Saraiva PP, Renno AC, et al. A novel bioactive vitroceramic presents similar biological responses as autogenous bone grafts. *J Mater Sci Mater Med.* 2012;23:1447–56. <https://doi.org/10.1007/s10856-012-4612-8>.
- Kido HW, Oliveira P, Parizotto NA, Crovace MC, Zanotto ED, Peitl-Filho O, et al. Histopathological, cytotoxicity and genotoxicity evaluation of Biosilicate(R) glass-ceramic scaffolds. *J Biomed Mater Res Part A.* 2013;101:667–73. <https://doi.org/10.1002/jbm.a.34360>.
- Kido HW, Brassolatti P, Tim CR, Gabbai-Armelin PR, Magri AM, Fernandes KR, et al. Porous poly (D,L-lactide-co-glycolide) acid/biosilicate(R) composite scaffolds for bone tissue engineering. *J Biomed Mater Res Part B Appl Biomater.* 2015;105:63–71. <https://doi.org/10.1002/jbm.b.33536>.
- Renno AC, Bossini PS, Crovace MC, Rodrigues AC, Zanotto ED, Parizotto NA. Characterization and *in vivo* biological performance of biosilicate. *BioMed Res Int.* 2013;2013:141427. <https://doi.org/10.1155/2013/141427>.
- Fernandes KR, Magri AMP, Kido HW, Ueno F, Assis L, Fernandes KPS, et al. Characterization and biological evaluation of the introduction of PLGA into biosilicate(R). *J Biomed Mater Res B Appl Biomater.* 2017;105:1063–74. <https://doi.org/10.1002/jbm.b.33654>.
- Välämäki VV, Aro HT. Molecular basis for the action of bioactive glasses as bone graft. *Scand J Surg.* 2006;95:95–102.

16. Hench LL, Xynos ID, Polak JM. Bioactive glasses for in situ tissue regeneration. *J Biomater Sci Polym Ed.* 2004;15:543–62. <https://doi.org/10.1163/156856204323005352>.
17. Rezwani K, Chen QZ, Blaker JJ, Boccaccini AR. Biodegradable and bioactive porous polymer/inorganic composite scaffolds for bone tissue engineering. *Biomaterials.* 2006;27:3413–31. <https://doi.org/10.1016/j.biomaterials.2006.01.039>.
18. Liao SS, Cui FZ, Zhang W, Feng QL. Hierarchically biomimetic bone scaffold materials: nano-HA/collagen/PLA composite. *J Biomed Mater Res Part B Appl Biomater.* 2004;69:158–65. <https://doi.org/10.1002/jbm.b.20035>.
19. Rizwan M, Hamdi M, Basirun WJ. Bioglass(R) 45S5-based composites for bone tissue engineering and functional applications. *J Biomed Mater Res Part A.* 2017;105:3197–223. <https://doi.org/10.1002/jbm.a.36156>.
20. Silva TH, Moreira-Silva J, Marques AL, Domingues A, Bayon Y, Reis RL. Marine origin collagens and its potential applications. *Mar drugs.* 2014;12:5881–901. <https://doi.org/10.3390/md12125881>.
21. Lin Z, Solomon KL, Zhang X, Pavlos NJ, Abel T, Willers C, et al. In vitro evaluation of natural marine sponge collagen as a scaffold for bone tissue engineering. *Int J Biol Sci.* 2011;7:968–77.
22. Gabbai-Armelin PR, Kido HW, Cruz MA, Prado JPS, Avanzi IR, Custodio MR, et al. Characterization and cytotoxicity evaluation of a marine sponge biosilica. *Mar Biotechnol.* 2019;21:65–75. <https://doi.org/10.1007/s10126-018-9858-9>.
23. Green D, Howard D, Yang X, Kelly M, Oreffo RO. Natural marine sponge fiber skeleton: a biomimetic scaffold for human osteoprogenitor cell attachment, growth, and differentiation. *Tissue Eng.* 2003;9:1159–66. <https://doi.org/10.1089/10763270360728062>.
24. Iwatsubo T, Kishi R, Miura T, Ohzono T, Yamaguchi T. Formation of hydroxyapatite skeletal materials from hydrogel matrices via artificial biomineralization. *J Phys Chem B.* 2015;119:8793–9. <https://doi.org/10.1021/acs.jpcc.5b03181>.
25. Exposito JY, Cluzel C, Garrone R, Lethias C. Evolution of collagens. *Anat Rec.* 2002;268:302–16. <https://doi.org/10.1002/ar.10162>.
26. Swatschek D, Schatton W, Kellermann J, Muller WE, Kreuter J. Marine sponge collagen: isolation, characterization and effects on the skin parameters surface-pH, moisture and sebum. *Eur J Pharm Biopharm.* 2002;53:107–13.
27. Lopez-Heredia MA, Sa Y, Salmon P, de Wijn JR, Wolke JG, Jansen JA. Bulk properties and bioactivity assessment of porous polymethylmethacrylate cement loaded with calcium phosphates under simulated physiological conditions. *Acta Biomater.* 2012;8:3120–7. <https://doi.org/10.1016/j.actbio.2012.05.007>.
28. Wang L, Yoon DM, Spicer PP, Henslee AM, Scott DW, Wong ME, et al. Characterization of porous polymethylmethacrylate space maintainers for craniofacial reconstruction. *J Biomed Mater Res Part B Appl Biomater.* 2013;101:813–25. <https://doi.org/10.1002/jbm.b.32885>.
29. Haach LCA, Purquerio BM, Silva NF Jr, Gaspar AMM, Fortulan CA. Comparison of two composites developed to be used as bone replacement—PMMA/bioglass 45S5<sup>®</sup> microfiber and PMMA/hydroxyapatite. *Bioceram Dev Appl.* 2014;4:71. <https://doi.org/10.4172/2090-5025.1000071>.
30. Shin H, Quinten Ruhe P, Mikos AG, Jansen JA. In vivo bone and soft tissue response to injectable, biodegradable oligo(poly(ethylene glycol) fumarate) hydrogels. *Biomaterials.* 2003;24:3201–11.
31. Parisi JR, Fernandes KR, Avanzi IR, Dorileo BP, Santana AF, Andrade AL, et al. Incorporation of collagen from marine sponges (Spongin) into hydroxyapatite samples: characterization and in vitro biological evaluation. *Mar Biotechnol.* 2019;21:30–7. <https://doi.org/10.1007/s10126-018-9855-z>.
32. Hutmacher DW, Schantz JT, Lam CX, Tan KC, Lim TC. State of the art and future directions of scaffold-based bone engineering from a biomaterials perspective. *J Tissue Eng Regen Med.* 2007;1:245–60. <https://doi.org/10.1002/term.24>.
33. Peitl O, Zanotto ED, Serbena FC, Hench LL. Compositional and microstructural design of highly bioactive P2O5-Na2O-CaO-SiO2 glass-ceramics. *Acta Biomater.* 2012;8:321–32. <https://doi.org/10.1016/j.actbio.2011.10.014>.
34. Oryan A, Baghaban Eslaminejad M, Kamali A, Hosseini S, Sayahpour FA, Baharvand H. Synergistic effect of strontium, bioactive glass and nano-hydroxyapatite promotes bone regeneration of critical-sized radial bone defects. *J Biomed Mater Res Part B Appl Biomater.* 2019;107:50–64. <https://doi.org/10.1002/jbm.b.34094>.
35. Lim HK, Byun SH, Woo JM, Kim SM, Lee SM, Kim BJ, et al. Biocompatibility and biocorrosion of hydroxyapatite-coated magnesium plate: animal experiment. *Materials.* 2017;10: 1149. <https://doi.org/10.3390/ma10101149>.
36. Liga Berzina-Cimdina and Natalija Borodajenko (April 25th 2012). Research of Calcium Phosphates using Fourier Transform Infrared Spectroscopy, *Infrared Spectroscopy - Materials Science, Engineering and Technology*, Theophile Theophanides, IntechOpen, DOI: 10.5772/36942. Available from: <https://www.intechopen.com/books/infrared-spectroscopy-materials-science-engineering-and-technology/research-of-calcium-phosphates-using-fourier-transformation-infrared-spectroscopy>.
37. Zdarta J, Norman LJ, Smulek W. Spongin-based scaffolds from *hippospongia communis* demosponge as an effective support for lipase immobilization. *Catalysts.* 2017;7:147.
38. Gabbai-Armelin PR, Souza MT, Kido HW, Tim CR, Bossini PS, Magri AM, et al. Effect of a new bioactive fibrous glassy scaffold on bone repair. *J Mater Sci Mater Med.* 2015;26:177. <https://doi.org/10.1007/s10856-015-5516-1>.
39. Gabbai-Armelin PR, Souza MT, Kido HW, Tim CR, Bossini PS, Fernandes KR, et al. Characterization and biocompatibility of a fibrous glassy scaffold. *J Tissue Eng Regen Med.* 2017;11:1141–51. <https://doi.org/10.1002/term.2017>.
40. Hench LL. The story of Bioglass. *J Mater Sci Mater Med.* 2006;17:967–78. <https://doi.org/10.1007/s10856-006-0432-z>.
41. Hench LL, Wilson J. An introduction to bioceramics. 2nd ed. London, U.K: Imperial College Press; 2013.
42. Deng L, Li D, Yang Z, Xie X, Kang P. Repair of the calvarial defect in goat model using magnesium-doped porous hydroxyapatite combined with recombinant human bone morphogenetic protein-2. *Bio-Med Mater Eng.* 2017;28:361–77. <https://doi.org/10.3233/BME-171678>.